

# Ultracold three-body collisions near overlapping Feshbach resonances

J. P. D’Incao<sup>1,2,3</sup> and B. D. Esry<sup>3</sup>

<sup>1</sup>*JILA, University of Colorado and NIST, Boulder, Colorado 80309-0440, USA*

<sup>2</sup>*Institut für Quantenoptik und Quanteninformation,*

*Österreichische Akademie der Wissenschaften, 6020 Innsbruck, Austria*

<sup>3</sup>*Department of Physics, Kansas State University, Manhattan, Kansas 66506, USA*

We present a comprehensive collection of ultracold three-body collisions properties near overlapping Feshbach resonances. Our results incorporate variations of all scattering lengths and demonstrate novel collisional behavior, such as atom-molecule interference effects. Taking advantage of the unique ways in which these collisions reflect Efimov physics, new pathways to control atomic and molecular losses open up. Further, we show that overlapping resonances can greatly improve the chances of observing multiple Efimov features in an ultracold quantum gas for nearly any system.

PACS numbers: 34.50.-s,67.85.-d,21.45.-v,31.15.xj

In the past few years, the experimental realization of ultracold gases with multiple species has made a whole new range of novel quantum phenomena experimentally accessible. In many cases, the underlying many-body physics depends on both intra- and inter-species correlations, emphasizing the importance of developing control over these types of interactions simultaneously. This control can be accomplished by applying an external magnetic field near values where two or more of the interactions support a Feshbach resonance [1], allowing for the various intra- and inter-species  $s$ -wave scattering lengths to vary drastically. Although such overlapping resonances can occur naturally, recent proposals [2] open up the possibility of controlling the interactions independently thus allowing the exploration of the multiple species strongly interacting regime. In this context, understanding the underlying few-body phenomena can potentially deepen the understanding of the many-body physics [3] as well as help to control the much more complex collisional behavior of the ultracold gas. In fact, recently, the first experimental studies on the collisional behavior of ultracold gases near overlapping Feshbach resonances [4] have revealed interesting universal few-body physics and triggered a number of theoretical studies [5].

The core of the few-body phenomena near overlapping Feshbach resonances is the extension of the three-body Efimov physics [6] to multiple large scattering lengths. Efimov physics and its manifestations in ultracold scattering near an isolated resonance is today well understood [7, 8]. When the scattering length  $a$  for identical bosons, for instance, is tuned to the universal regime  $|a| \gg r_0$ , where  $r_0$  is the range of the two-body interactions, loss rates reveal signatures of Efimov states as seen in the fast-growing number of experiments [9, 10], demonstrating the importance of universal few-body physics [11].

In this Letter, we will show that when multiple scattering lengths are allowed to vary, the signatures of Efimov physics in scattering observables are much richer than the single scattering length cases and open up new fronts for the control of atomic and molecular losses.

We have found, for instance, that when two scattering lengths are large and positive, Efimov physics can cause destructive interference in atom-molecule collisions, allowing for longer molecular lifetimes, even in the absence of Pauli blocking [12]. In other cases we show that both destructive and constructive interference can be observed in the *same* scattering process unlike the single resonance case. Importantly for few-body physics, we show that near overlapping resonances the strength of the effective three-body interaction behind the Efimov effect can be made much stronger and thus improve the observability of the Efimov effect in a great variety of systems. In fact, it turns out that the Efimov effect is easier to observe in *any* system with overlapping resonances than in identical boson systems. We also derive the scattering length dependence for the important inelastic scattering processes in systems consisting of two identical bosons and a dissimilar particle, say  $BBX$ , and three dissimilar particles, say  $XYZ$ , with two and three resonant scattering lengths. The latter is relevant for the recent experiments with  ${}^6\text{Li}$  in three different spin states [4].

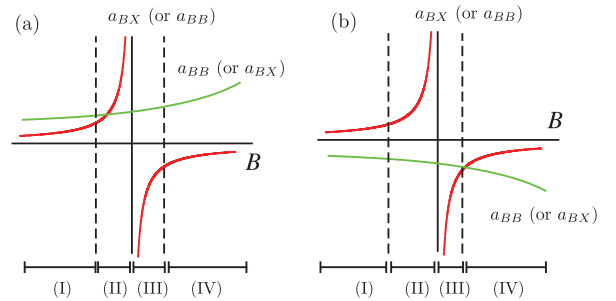


FIG. 1: (color online). Idealized picture for two overlapping  $s$ -wave Feshbach resonances between  $B$  and  $X$  atomic species, focusing on just one of the resonances. In (a) there are one or two weakly bound molecular states, and in (b) zero or one molecular state can exist. The regions (I)–(IV) in each case exhaust all scenarios in general.

We start our study of three-body physics near overlap-

ping Feshbach resonances by identifying the most generic cases. In Fig. 1 we show these cases for two nearby resonances between  $B$  and  $X$  atomic species, focusing only on the region around one of the resonances. Figure 1(a) illustrates the case where one of the scattering lengths goes through a pole while the other remains large and positive, while in Fig. 1(b) the pole occurs when the other scattering length is large and negative. The main difference between these two cases is that in Fig. 1(a) there exist two weakly bound molecular states  $BB^*$  and  $BX^*$ , associated with the scattering lengths  $a_{BB}$  and  $a_{BX}$ , respectively, while in Fig. 1(b) only one weakly bound  $BX^*$  molecular state exists. Even though the cases shown in Fig. 1 are only an idealization of the overlap between two resonances, the four regions labeled in each case—where our results and analysis are applied separately—exhaust all possibilities for two overlapping resonances.

Our results for the three-body inelastic rates are derived from the generalization of our methodology [7] to multiple scattering lengths. The key ingredient in our approach is that the scattering length dependence of the rates is determined by a combination of tunneling through effective three-body potential barriers and interference effects [7]. The form of the effective potentials thus controls the collisional properties of the system. In the adiabatic hyperspherical representation, the effective three-body potentials can be parameterized as

$$W_\nu(R) = -\frac{s_0^2 + 1/4}{2\mu R^2} \quad \text{and} \quad W_\nu(R) = \frac{p_0^2 - 1/4}{2\mu R^2}, \quad (1)$$

for attractive and repulsive Efimov potentials, respectively, in each region  $r_0 \ll R \ll |a'|$  and  $|a'| \ll R \ll |a|$ , assuming  $|a| \gg |a'|$ . Here,  $R$  is the hyperradius describing the overall size of the system,  $\mu$  is the three-body reduced mass [7] and  $\nu$  the set of quantum numbers necessary to label each channel. The strengths of the attractive and repulsive interactions  $s_0$  and  $p_0$ , respectively, as well as the systems in which they occur, are dictated by Efimov physics [7, 8] through the values of the mass ratios between the particles and whether they are of bosonic or fermionic character. We note that  $s_0$  and  $p_0$  also depend on the number of resonant interactions and will thus be different in each  $R$  region. For instance, for three identical bosons—where all the pairs interact resonantly—the attractive potential in Eq. (1) has  $s_0 \approx 1.00624$ . On the other hand, for systems with three bosons in two different spin states and resonant interspecies interaction—giving two resonantly interacting pairs— $s_0 \approx 0.41370$ . Now, if the intraspecies interaction in the above example is also resonant, the value for  $s_0$  is the same as for three identical bosons. The same values are also obtained for particles in three different spin states relevant to Refs. [3, 4].

Because of their effect on  $s_0$ , overlapping resonances can have a significant impact on the observation of Efimov physics. In fact, one of the major obstacles for observing the Efimov effect through ultracold scattering is

that the loss features occur at scattering lengths separated by the multiplicative factor  $e^{\pi/s_0}$ . Therefore, observing  $n$  features requires the ability to change  $a$  by roughly a factor of  $(e^{\pi/s_0})^n = 22.7^n$  for identical bosons. Although a much smaller value for  $e^{\pi/s_0}$  can be obtained by choosing appropriate mass ratios [7], this approach severely limits the number of favorable systems. Near overlapping resonances, however, the situation is drastically improved. In Fig. 2 we show  $s_0$  and  $e^{\pi/s_0}$  for  $BBX$  systems where only  $a_{BX}$  is resonant, i.e., for an isolated resonance. As can be seen, scaling factors more favorable than for identical bosons are obtained only for mass ratios  $\delta = m_X/m_B$  less than approximately 0.2. For larger  $\delta$ ,  $e^{\pi/s_0}$  diverges, making it unlikely that even a single Efimov feature could be observed. In contrast, for multiple large scattering lengths,  $s_0^*$  and  $e^{\pi/s_0^*}$ —also shown in Fig. 2 [6]—substantially improve on the identical boson case for *all* mass ratios. Therefore, overlapping resonances dramatically enhance the feasibility of observing the Efimov effect in a greater variety of systems.

In Tables I and II (see Ref. [13]), we summarize our major results for the collisional rates for  $BBX$  and  $XYZ$  systems. In Table I, we assume that only two of the scattering lengths are resonant, while in Table II all three scattering lengths are resonant. For atom-molecule collisions, Table I gives the rate constants for vibrational relaxation, represented generically by  $XY^* + Z \rightarrow XY + Z$ ,  $V_{\text{rel}}$ , and for reactive scattering,  $XY^* + Z \rightarrow XZ^* + Y$ , denoted by  $\beta$ . For collisions involving three atoms, we give the loss rate for three-body recombination,  $K_3$ , one example of which is given by  $X + Y + Z \rightarrow XY^* + Z$ . In Tables I and II the modulation factors  $M$  and  $P$  are

$$M_{s_0}\left(\frac{x}{y}\right) \propto \sin^2[s_0 \ln(|\frac{x}{y}|) + \Phi] + \sinh^2\eta, \quad (2)$$

$$P_{s_0}\left(\frac{x}{y}\right) \propto \frac{\sinh 2\eta}{\sin^2[s_0 \ln(|\frac{x}{y}|) + \Phi] + \sinh^2\eta}, \quad (3)$$

$$M_{s_0^*}\left(\frac{x}{y}, \frac{z}{u}\right) \propto \sin^2[s_0 \ln(|\frac{x}{y}|) + s_0^* \ln(|\frac{z}{u}|) + \Phi] + \sinh^2\eta, \quad (4)$$

$$P_{s_0^*}\left(\frac{x}{y}, \frac{z}{u}\right) \propto \frac{\sinh 2\eta}{\sin^2[s_0 \ln(|\frac{x}{y}|) + s_0^* \ln(|\frac{z}{u}|) + \Phi] + \sinh^2\eta}, \quad (5)$$

and provide the signatures of Efimov physics. In these expressions  $\Phi$  is an unknown phase that determines the positions of the interference minima (in the  $M$ 's) and the resonant peaks associated with the creation of an Efimov state ( $P$ 's), and  $\eta$  is a parameter associated with the probability to decay to deeply bound states. Both  $\Phi$  and  $\eta$  are non-universal short-range three-body parameters that must, with the current theoretical limitations, be determined for each system empirically.

In contrast to isolated resonances, where interference minima only occur in  $K_3$  ( $a > 0$ ) and resonant enhancements only occur in  $K_3$  ( $a < 0$ ) and  $V_{\text{rel}}$  ( $a > 0$ ), minima and peaks appear ubiquitously near overlapping resonances and, in some cases, both can happen in the

TABLE I: Scattering length dependence for three-body collision rates in  $BBX$  and  $XYZ$  systems. For  $BBX$  systems both  $a_{BX}$  and  $a_{BB}$  scattering lengths are resonant, while for  $XYZ$  systems only  $a_{XY}$  and  $a_{XZ}$  are resonant. The notation  $|a|$  indicates  $a < 0$ , and no entry indicates that the associated process is not possible. Expressions for  $M$  and  $P$  are given in Eqs. (2)–(5).

	$a_{BX} \ll a_{BB}$	$a_{BX} \gg a_{BB}$	$ a_{BX}  \gg a_{BB}$	$ a_{BX}  \ll a_{BB}$
$BX^* + B \rightarrow BB^* + X$	—	$P_{s_0^*}(\frac{a_{BX}}{a_{BB}})M_{s_0}(\frac{a_{BB}}{r_0})a_{BX}$	—	—
$\rightarrow BB + X, BX + B$	$P_{s_0}(\frac{a_{BX}}{r_0})a_{BX}$	$P_{s_0^*}(\frac{a_{BX}}{a_{BB}})a_{BX}$	—	—
$BB^* + X \rightarrow BX^* + B$	$M_{s_0}(\frac{a_{BX}}{r_0})a_{BX}^2/a_{BB}$	—	—	—
$\rightarrow BB + X, BX + B$	$a_{BX}^2/a_{BB}$	$P_{s_0^*}(\frac{a_{BB}}{r_0})a_{BB}$	$P_{s_0^*}(\frac{a_{BB}}{r_0})a_{BB}$	$P_{s_0}(\frac{a_{BX}}{r_0})a_{BX}^2/a_{BB}$
$B + B + X \rightarrow BX^* + B$	$M_{s_0}(\frac{a_{BX}}{r_0})a_{BX}^2a_{BB}^2$	$M_{s_0^*}(\frac{a_{BB}}{a_{BB}})a_{BB}^4$	—	—
$\rightarrow BB^* + X$	$a_{BB}^4$	$M_{s_0}(\frac{a_{BB}}{r_0})a_{BB}^4$	$P_{s_0^*}(\frac{a_{BB}}{a_{BB}})M_{s_0}(\frac{a_{BB}}{r_0})a_{BB}^4$	$a_{BB}^4$
$\rightarrow BB + X, BX + B$	$a_{BX}^2a_{BB}^2$	$a_{BX}^4$	$P_{s_0^*}(\frac{a_{BX}}{a_{BB}})a_{BX}^4$	$a_{BX}^2a_{BB}^2$
	$a_{BX} \ll  a_{BB} $	$a_{BX} \gg  a_{BB} $	$ a_{BX}  \gg  a_{BB} $	$ a_{BX}  \ll  a_{BB} $
$BX^* + B \rightarrow BB + X, BX + B$	$P_{s_0}(\frac{a_{BX}}{r_0})a_{BX}$	$P_{s_0^*}(\frac{a_{BB}}{r_0}, \frac{a_{BX}}{a_{BB}})a_{BX}$	—	—
$B + B + X \rightarrow BX^* + B$	$M_{s_0}(\frac{a_{BX}}{r_0})a_{BX}^2a_{BB}^2$	$M_{s_0^*}(\frac{a_{BB}}{r_0}, \frac{a_{BX}}{a_{BB}})a_{BB}^4$	—	—
$\rightarrow BB + X, BX + B$	$a_{BX}^2a_{BB}^2$	$a_{BX}^4$	$P_{s_0^*}(\frac{a_{BB}}{r_0}, \frac{a_{BX}}{a_{BB}})a_{BB}^4$	$P_{s_0}(\frac{a_{BX}}{r_0})a_{BX}^2a_{BB}^2$
	$a_{XY} \gg a_{XZ}$	$ a_{XY}  \gg a_{XZ}$	$a_{XY} \gg  a_{XZ} $	$ a_{XY}  \gg  a_{XZ} $
$XY^* + Z \rightarrow XZ^* + Y$	$M_{s_0}(\frac{a_{XZ}}{r_0})a_{XZ}^2/a_{XY}$	—	—	—
$\rightarrow XY + Z, XZ + Y, \dots$	$a_{XZ}^2/a_{XY}$	—	$P_{s_0}(\frac{a_{XZ}}{r_0})a_{XZ}^2/a_{XY}$	—
$XZ^* + Y \rightarrow XY + Z, XZ + Y, \dots$	$P_{s_0}(\frac{a_{XZ}}{r_0})a_{XZ}$	$P_{s_0}(\frac{a_{XZ}}{r_0})a_{XZ}$	—	—
$X + Y + Z \rightarrow XY^* + Z$	$a_{XY}^4$	—	$a_{XY}^4$	—
$\rightarrow XZ^* + Y$	$M_{s_0}(\frac{a_{XZ}}{r_0})a_{XZ}^2a_{XY}^2$	$M_{s_0}(\frac{a_{XZ}}{r_0})a_{XZ}^2a_{XY}^2$	—	—
$\rightarrow XY + Z, XZ + Y, \dots$	$a_{XZ}^2a_{XY}^2$	$a_{XZ}^2a_{XY}^2$	$a_{XZ}^2a_{XY}^2$	$P_{s_0}(\frac{a_{XZ}}{r_0})a_{XZ}^2a_{XY}^2$

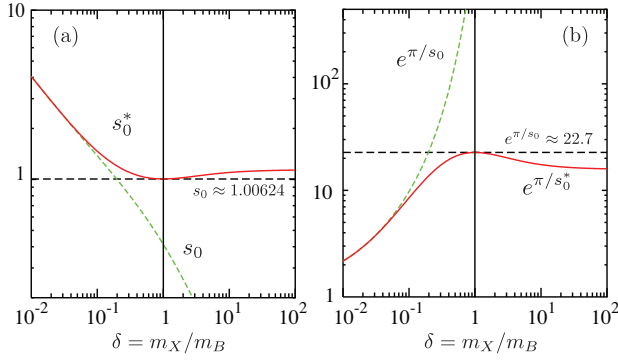


FIG. 2: (color online). Effect of overlapping resonances on (a) the strength of the Efimov potential  $s_0$  [see Eq. (1)] and (b) the scale factor  $e^{\pi/s_0}$  separating Efimov features as a function of  $a$ . Both panels include the results for large scattering lengths between two ( $s_0$ , green dashed line) and three ( $s_0^*$ , red solid line) pairs of particles.

*same* scattering process. This result reflects the complexity of scattering near overlapping resonances and opens up many alternatives for observing Efimov physics and achieving atomic and molecular stability.

We expect the formulas in Tables I and II to apply in the threshold regime [14] —i.e., for energies (temperatures) smaller than  $1/(2\mu_{BB}a_{BB}^2)$  and  $1/(2\mu_{BX}a_{BX}^2)$ ,

where  $\mu_{ij}$  is the two-body reduced mass— and when the scattering lengths differ from each other by an order of magnitude or more. Otherwise, the effective potentials will not distinctly display the regions in  $R$  discussed above. In this case, one should assume that two similar scattering lengths are equal in magnitude for the purpose of using Tables I and II.

In Fig. 3 we single out two interesting cases from Table I. Figure 3(a) shows the interference effects in  $BB^* + X \rightarrow BX^* + B$  collisions ( $a_{BB} \gg a_{BX}$ ), and Fig. 3(b) shows the rate for  $BX^* + B \rightarrow BB^* + X$  collisions ( $a_{BX} \gg a_{BB}$ ), displaying *both* interference minima and resonant effects—the latter is due to the appearance of Efimov states at the  $BX^* + B$  threshold. For the examples in Fig. 3(a) and (b), we have chosen an arbitrary  $a_{BB}$  and  $a_{BX}$  dependence on the  $B$ -field that allows both scattering lengths to vary substantially and to display more than one Efimov feature—note that we also have chosen an arbitrary phase  $\Phi$  for the position of the Efimov features in Eqs. (2)–(5) as well as a small  $\eta$  to make such features more pronounced. For more realistic systems, decay to deeply bound molecules would increase  $\eta$ , possibly limiting the observability of the interference minima. In the experiments to date, however,  $\eta$  has tended to be small. Nevertheless, it is interesting to notice that in both cases, if the  $a_{BB}$  and  $a_{BX}$  can be

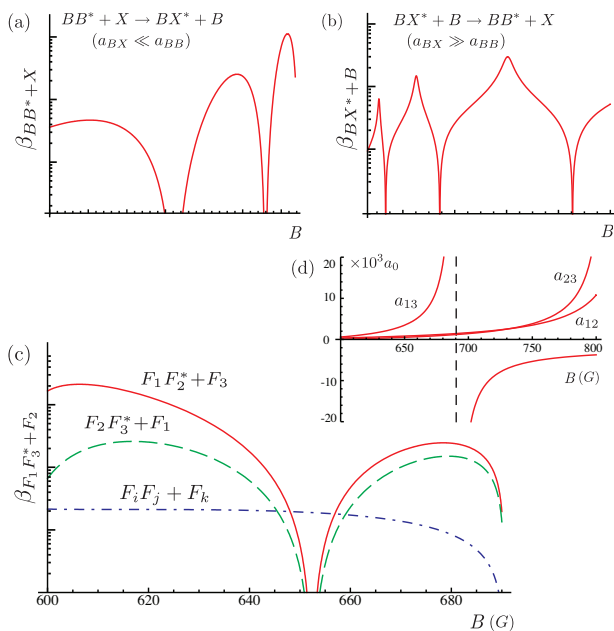


FIG. 3: (color online) The magnetic field dependence of selected processes using the present results. Reactive scattering showing (a) interference minima and (b) both interference minima and resonant enhancement. (c) Atom-molecule collision rates for three-spin mixtures of  ${}^6\text{Li}$  [4] for the region in (d) where all three scattering lengths are large and positive.

controlled independently [2], one of them can be adjusted to a minimum in  $M$  leading to the overall suppression of the losses as a function of the other scattering length.

In Fig. 3(c) we apply our results to the case of the three overlapping resonances in  ${}^6\text{Li}$  [4] in the range of  $B$ -field where the three scattering lengths  $a_{12}$ ,  $a_{13}$ , and  $a_{23}$ , are all large and positive [see Fig 3(d)]. From our results in Table II (see Ref. [13]), we have found that relaxation of  $F_1 F_3^*$  molecules due to collisions with  $F_2$  atoms is suppressed as  $a_{13} \rightarrow \infty$ . Specifically, we found the rates for the processes  $F_1 F_3^* + F_2 \rightarrow F_1 F_2^* + F_3$ ,  $F_2 F_3^* + F_1$  and  $F_i F_j + F_k$  (where  $F_i F_j$  is a deeply bound molecule), to be  $M_{s_0} (a_{23}/r_0) a_{12}^2/a_{13}$ ,  $M_{s_0} (a_{23}/r_0) a_{23}^2/a_{13}$ , and  $a_{23}^2/a_{13}$ , respectively, displaying a  $a_{13}^{-1}$  suppression. These expressions show that  $F_1 F_3^* + F_2$  collisions can also display interference effects associated with Efimov physics [see Fig. 3(c)]. The precise location of the minimum, however, will depend on the short-range three-body physics. Therefore, we can only conclude that for this region of  $B$ -fields the scattering lengths change enough to produce a minimum.

In summary, we show that despite the great increase in complexity, the scattering length dependence of the ultracold three-body rates near overlapping resonances can be understood. The effect of such overlaps expands the ways in which Efimov physics can be observed and introduces new effects such as atom-molecule interference

minima. We also show that overlapping resonances reduce the geometric spacing of Efimov features compared to identical bosons for essentially all possible three-body systems with arbitrary masses.

This work was supported by the National Science Foundation.

- 
- [1] A. Simoni *et al.* Phys. Rev. Lett. **90**, 163202 (2003); M. Bartenstein *et al.*, *ibid.* **94**, 103201 (2005)
  - [2] D. M. Bauer, *et al.*, Nature Phys. **5**, 339 (2009); B. Marcellis, B. Verhaar, and S. Kokkelmans, Phys. Rev. Lett. **100**, 153201 (2008).
  - [3] C. Honerkamp and W. Hofstetter, Phys. Rev. B **70**, 094521 (2004); A. Rapp, W. Hofstetter and G. Zaránd, *ibid.* **77**, 144520 (2008); R. W. Cherng, G. Refael, and E. Demler, Phys. Rev. Lett. **99**, 130406 (2007); A. Rapp *et al.*, *ibid.* **98**, 160405 (2007); T. Paananen, P. Torma, and J.-P. Martikainen, Phys. Rev. A **73**, 053606 (2006); *ibid.* **75**, 023622 (2007); H. Zhai, *ibid.* **75**, 031603(R) (2007); G. Catelani and E. A. Yuzbashyan, *ibid.* **78**, 033615 (2008); P. F. Bedaque, J. P. D’Incao, Ann. of Phys. **324**, 1736 (2009).
  - [4] T. B. Ottenstein *et al.*, Phys. Rev. Lett. **101**, 203202 (2008); J. H. Huckans *et al.*, *ibid.* **102**, 165302 (2009).
  - [5] E. Braaten *et al.*, arXiv:0811.3578; P. Naidon and M. Ueda, arXiv:0811.4086; R. Schmidt, S. Floerchinger, C. Wetterich arXiv:0812.1191v1.
  - [6] V. Efimov, Yad. Fiz. **12**, 1080 (1970) [Sov. J. Nucl. Phys. **12**, 589 (1971)]; V. Efimov, JETP Letters **16**, 50 (1972); Nucl. Phys. A **210**, 157 (1973).
  - [7] J. P. D’Incao and B. D. Esry, Phys. Rev. Lett. **94**, 213201 (2005); Phys. Rev. A **73**, 030702(R) (2006).
  - [8] E. Braaten and H.-W. Hammer, Phys. Rep. **428**, 259 (2006).
  - [9] T. Kraemer *et al.*, Nature (London) **440**, 315 (2006); S. Knoop *et al.*, Nature Phys. **5**, 227 (2009); G. Barontini *et al.*, arXiv:0901.4584; M. Zaccanti, *et al.*, arXiv:0904.4453.
  - [10] F. Ferlaino *et al.*, Phys. Rev. Lett. **101**, 023201 (2008); F. Ferlaino *et al.*, *ibid.* **102**, 140401 (2009).
  - [11] L. Platter, H.-W. Hammer, and Ulf-G. Meißner, Phys. Rev. A **70**, 052101 (2004). G. J. Hanna and D. Blume, *ibid.* **74**, 063604 (2006); M. Yamashita *et al.*, Europhys. Lett. **75**, 555 (2006); H. Hammer and L. Platter, Eur. Phys. J. A **32**, 113 (2007); Y. Wang and B. D. Esry, Phys. Rev. Lett. **102**, 133201 (2009); J. von Stecher, J. P. D’Incao, and C. H. Greene, Nature Phys. **5**, 417; J. P. D’Incao, J. von Stecher, and C. H. Greene, to appear in Phys. Rev. Lett., arXiv:0903.3348
  - [12] D. S. Petrov, C. Salomon, and G. V. Shlyapnikov, Phys. Rev. Lett. **93**, 090404 (2004); J. P. D’Incao and B. D. Esry, *ibid.* **100**, 163201(R) (2008). J. P. D’Incao, *et al.*, Phys. Rev. A **79**, 030501 (2009).
  - [13] See EPAPS Document No. [will be inserted by publisher].
  - [14] J. P. D’Incao, H. Suno and B. D. Esry, Phys. Rev. Lett. **93**, 123201 (2004); J. P. D’Incao, Chris H. Greene, and B. D. Esry, J. Phys. B **42**, 044016 (2009).

TABLE II: Scattering length dependence for three-body collision rates in  $XYZ$  systems with three large scattering lengths, i.e., for  $|a_{XY}| \gg r_0$ ,  $|a_{XZ}| \gg r_0$ , and  $|a_{YZ}| \gg r_0$ . The notation  $|a|$  indicates  $a < 0$ , and no entry indicates that the associated process is not possible. Expressions for  $M$  and  $P$  are given in Eqs. (2)–(5) of the main text.

	$a_{XY} \gg a_{XZ} \gg a_{YZ}$	$ a_{XY}  \gg a_{XZ} \gg a_{YZ}$	$a_{XY} \gg  a_{XZ}  \gg a_{YZ}$	$a_{XY} \gg a_{XZ} \gg  a_{YZ} $
$XY^*+Z \rightarrow XZ^*+Y$	$M_{s_0}(\frac{a_{XZ}}{a_{YZ}})a_{XZ}^2/a_{XY}$	—	—	$M_{s_0}^{s_0^*}(\frac{a_{YZ}}{r_0}, \frac{a_{XZ}}{a_{YZ}})a_{XZ}^2/a_{XY}$
$\rightarrow YZ^*+X$	$M_{s_0}^{s_0^*}(\frac{a_{YZ}}{r_0})a_{XZ}^2/a_{XY}$	—	$P_{s_0}(\frac{a_{XZ}}{a_{YZ}})M_{s_0}^{s_0^*}(\frac{a_{YZ}}{r_0})\frac{a_{XZ}^2}{a_{XY}}$	—
$\rightarrow XY+Z, XZ+Y, \dots$	$a_{XZ}^2/a_{XY}$	—	$P_{s_0}(\frac{a_{XZ}}{a_{YZ}})a_{XZ}^2/a_{XY}$	$a_{XZ}^2/a_{XY}$
$XZ^*+Y \rightarrow YZ^*+X$	$P_{s_0}(\frac{a_{XZ}}{a_{YZ}})M_{s_0}^{s_0^*}(\frac{a_{YZ}}{r_0})a_{XZ}$	$P_{s_0}(\frac{a_{XZ}}{a_{YZ}})M_{s_0}^{s_0^*}(\frac{a_{YZ}}{r_0})a_{XZ}$	—	—
$\rightarrow XY+Z, XZ+Y, \dots$	$P_{s_0}(\frac{a_{XZ}}{a_{YZ}})a_{XZ}$	$P_{s_0}(\frac{a_{XZ}}{a_{YZ}})a_{XZ}$	—	$P_{s_0}^{s_0^*}(\frac{a_{YZ}}{r_0}, \frac{a_{XZ}}{a_{YZ}})a_{XZ}$
$YZ^*+X \rightarrow XY+Z, XZ+Y, \dots$	$P_{s_0}^{s_0^*}(\frac{a_{YZ}}{r_0})a_{YZ}$	$P_{s_0}^{s_0^*}(\frac{a_{YZ}}{r_0})a_{YZ}$	$P_{s_0}^{s_0^*}(\frac{a_{YZ}}{r_0})a_{YZ}$	—
$X+Y+Z \rightarrow XY^*+Z$	$a_{XY}^4$	—	$a_{XY}^4$	$a_{XY}^4$
$\rightarrow XZ^*+Y$	$M_{s_0}(\frac{a_{XZ}}{a_{YZ}})a_{XZ}^2a_{XY}^2$	$M_{s_0}(\frac{a_{XZ}}{a_{YZ}})a_{XZ}^2a_{XY}^2$	—	$M_{s_0}^{s_0^*}(\frac{a_{YZ}}{r_0}, \frac{a_{XZ}}{a_{YZ}})a_{XZ}^2a_{XY}^2$
$\rightarrow YZ^*+X$	$M_{s_0}^{s_0^*}(\frac{a_{YZ}}{r_0})a_{XZ}^2a_{XY}^2$	$M_{s_0}^{s_0^*}(\frac{a_{YZ}}{r_0})a_{XZ}^2a_{XY}^2$	$M_{s_0}^{s_0^*}(\frac{a_{YZ}}{r_0})a_{XZ}^2a_{XY}^2$	—
$\rightarrow XY+Z, XZ+Y, \dots$	$a_{XZ}^2a_{XY}^2$	$a_{XZ}^2a_{XY}^2$	$a_{XZ}^2a_{XY}^2$	$a_{XZ}^2a_{XY}^2$
	$ a_{XY}  \gg  a_{XZ}  \gg a_{YZ}$	$a_{XY} \gg  a_{XZ}  \gg  a_{YZ} $	$ a_{XY}  \gg a_{XZ} \gg  a_{YZ} $	$ a_{XY}  \gg  a_{XZ}  \gg  a_{YZ} $
$XY^*+Z \rightarrow XZ^*+Y$	—	—	—	—
$\rightarrow YZ^*+X$	—	—	—	—
$\rightarrow XY+Z, XZ+Y, \dots$	—	$P_{s_0}^{s_0^*}(\frac{a_{YZ}}{r_0}, \frac{a_{XZ}}{a_{YZ}})a_{XZ}^2/a_{XY}$	—	—
$XZ^*+Y \rightarrow YZ^*+X$	—	—	—	—
$\rightarrow XY+Z, XZ+Y, \dots$	—	—	$P_{s_0}^{s_0^*}(\frac{a_{YZ}}{r_0}, \frac{a_{XZ}}{a_{YZ}})a_{XZ}$	—
$YZ^*+X \rightarrow XY+Z, XZ+Y, \dots$	$P_{s_0}^{s_0^*}(\frac{a_{YZ}}{r_0})a_{YZ}$	—	—	—
$X+Y+Z \rightarrow XY^*+Z$	—	$a_{XY}^4$	—	—
$\rightarrow XZ^*+Y$	—	—	—	—
$\rightarrow YZ^*+X$	$P_{s_0}(\frac{a_{XZ}}{a_{YZ}})M_{s_0}^{s_0^*}(\frac{a_{YZ}}{r_0})a_{XZ}^2a_{XY}^2$	—	$M_{s_0}^{s_0^*}(\frac{a_{YZ}}{r_0}, \frac{a_{XZ}}{a_{YZ}})a_{XZ}^2a_{XY}^2$	—
$\rightarrow XY+Z, XZ+Y, \dots$	$P_{s_0}(\frac{a_{XZ}}{a_{YZ}})a_{XZ}^2a_{XY}^2$	$a_{XY}^4$	$a_{XZ}^2a_{XY}^2$	$P_{s_0}^{s_0^*}(\frac{a_{YZ}}{r_0}, \frac{a_{XZ}}{a_{YZ}})a_{XZ}^2a_{XY}^2$